Loss of Microtubule Associated Protein 2 Immunoreactivity Linked to Dendritic Spine Loss in Schizophrenia

by

Micah Aaron Shelton

Bachelor of Arts, McDaniel College, Westminster, MD 2011

Submitted to the Graduate Faculty of

University of Pittsburgh in partial fulfillment

of the requirements for the degree of

Master of Science

University of Pittsburgh

2015

UNIVERSITY OF PITTSBURGH

School of Medicine

This thesis was presented

by

Micah Aaron Shelton

It was defended on

August 17th, 2015

and approved by

Kenneth N. Fish, PhD, Department of Psychiatry

Susan R. Sesack, PhD, Department of Neurobiology

Thesis Advisor: Robert A. Sweet, MD, Department of Psychiatry

Loss of Microtubule Associated Protein 2 Immunoreactivity Linked to Dendritic Spine Loss in Schizophrenia

Micah A. Shelton M.S.

University of Pittsburgh, 2015

Microtubule-associated protein 2 (MAP2) is a neuronal protein that plays a role in maintaining dendritic structure through its interaction with microtubules. In schizophrenia (Sz), a number of studies have revealed that MAP2's typically robust immunoreactivity (IR) is significantly reduced across several cortical regions. Previous studies have not explored the relationship between MAP2-IR reduction and lower dendritic spine density, which is frequently reported in schizophrenia nor has MAP2-IR loss been investigated in the primary auditory cortex (Brodmann Area 41), a site of conserved pathology in Sz. Last, the impact of chronic antipsychotic exposure is little understood. Using quantitative spinning disk confocal microscopy in two cohorts of Sz subjects and matched control subjects (Sz, n=20; C, n=20), we measured MAP2-IR as well as dendritic spine density and spine number in deep layer 3 of BA41. Sz subjects exhibited a significant reduction in MAP2-IR. The reductions in MAP2-IR were not associated with neuron loss, loss of MAP2 protein, clinical confounds, or technical factors; nor were MAP2-IR reductions linked with chronic haloperidol exposure in a macaque model. Dendritic spine density and number were also reduced in Sz and correlated with MAP2-IR. Twelve (60%) Sz subjects exhibited MAP2-IR values lower than the lowest controls; only in this group were spine density and number significantly reduced. These findings demonstrate that MAP2-IR loss is closely linked to dendritic spine pathology in Sz. Because MAP2 shares substantial sequence, regulatory, and functional homology with MAP tau, the wealth of

knowledge regarding tau biology and the rapidly expanding field of tau therapeutics provide resources for identifying how MAP2 is altered in Sz and possible leads to novel therapeutics.

TABLE OF CONTENTS

LIST OF TABLES

LIST OF FIGURES

PREFACE

This work was supported by grants DC011499-03(MAS), MH16804 (MLM), MH096985 (KNF), MH071316 and MH097216 (PP) and MH071533 (RAS). I would like to thank Dr. C. Sue Johnston for assistance with the clinical data, Mary Brady for design assistance, and the research staff of the Translational Neuroscience Program for technical assistance. The Biomedical Mass Spectrometry Center and UPCI Cancer Biomarker Facility are supported in part by award P30CA047904. I would like to thank my thesis advisor Dr. Robert Sweet for his guidance and willingness to teach; his selflessness, patience and compassion have been instrumental in my maturation as a person and as a scientist.

1.0 GENERAL INTRODUCTION

Portions of this thesis have been presented in abstract form, including:

Shelton MA, Newman JT, Fish KN, Penzes P, Lewis DA, Sweet RA. “Loss of Microtubule Associated Protein 2 Immunoreactivity Linked to Dendritic Spine Loss in Schizophrenia.” Program No. 254.16. 2013 Neuroscience Meeting Planner. San Diego, CA: Society for Neuroscience, 2013. Online.

Shelton MA, Newman JT, Gu H, Sampson AR, Fish KN, Penzes PP, Lewis DA, Sweet RA. “Haloperidol-exposure does not affect schizophrenia-liked reductions in microtubule associated protein 2 immunoreactivity. Program No. 229.19. 2014 Neuroscience Meeting Planner. Washington D.C.: Society for Neuroscience, 2014. Online.

Portions of this thesis have been presented as published manuscript:

Shelton MA, Newman JT, Gu H, Sampson AR, Fish KN, MacDonald ML, Moyer CE, DiBitetto JV, Dorph-Petersen KA, Penzes PP, Lewis DA, Sweet RA. Loss of Microtubule Associated Protein 2 Immunoreactivity Linked to Dendritic Spine Loss in Schizophrenia. 2015 Jan 30 Biological Psychiatry.

2.0 SCHIZOPHRENIA: EPIDEMIOLOGY AND ETIOPATHOLOGY

2.1 PREVALENCE AND PRESENTATION

Schizophrenia (Sz) is a devastating, progressive psychiatric disorder that affects between 0.5-1% of the global population (Jablensky 2000) . Most individuals present with symptoms during late adolescence and early adulthood, generally between the ages of 18 and 30, a period of rapid cortical development and social, occupational, and educational transition (Moyer et al 2015). During this time of developmental sensitivity, stressful life events can produce psychiatric pathology in genetically vulnerable individuals. Males typically have an earlier age of onset, a higher lifetime risk of developing Sz, and tend to have a poorer prognosis overall. Though, for all afflicted, Sz incurs a considerable interpersonal cost in terms of lost educational and employment opportunities, difficulties in managing social relationships, and maintaining independent self-care. The clinical population experiences a shortening of general life expectancy compared to the general population of between two to three decades, partly attributable to increased rates of substance abuse and suicide but also due to a greater incidence of comorbid cardiovascular disease (Lewis and Sweet 2009, Moyer et al 2015, Salyers and Mueser 2001, Tiihonen et al 2009).

While highly heterogeneous, the disorder is characterized by a pattern of symptomology divided into three major domains: positive, negative, and cognitive. Positive symptoms, also

referred to as psychotic symptoms, are abnormal functions which distort reality. Hallucinations, especially auditory verbal hallucinations, are classically associated with Sz. However, positive symptomology extends beyond a distortion in the normal perception of the external world and includes a parallel distortion in the production of normal thought, speech, and psychomotor activity. This often manifests in delusional thinking, false beliefs, loose associations, over-inclusiveness, and neologisms (i.e. the creation of new words or expressions). Psychomotor impairments are expressed as grossly disorganized behavior and posturing. While positive symptoms may be conceived as the addition of abnormal functions, negative symptoms describe a loss of normal functions. Negative symptoms include alogia (i.e. poverty in speech production), avolition (i.e. a deficit in motivation), and anhedonia (i.e. a deficit in the ability to experience pleasure) (Chapman 1966, Lewis and Sweet 2009).

Cognitive symptoms are deficits in higher executive function including attention, working and episodic memory, impulse control, and social engagement. Evidence places the cognitive symptomology at the core of the disorder. The degree of cognitive symptomology is relatively stable over the course of the disorder and is independent from the severity of positive symptoms. Cognitive deficits are present during developmental stages prior to diagnosis and become overt during the first clinical presentation. The large majority of Sz patients (i.e. between 75%-85%) perform 1-3 standard deviations below control subjects on tests of specific neuropsychological abilities such as attention, learning, memory, and abstraction. This finding holds true both for chronic Sz patients and for neuroleptic naive individuals assessed at their first-episode of psychosis. Retrospective studies of Sz patients which compare their academic performance to that of their peers prior to disease onset, show that individuals who go on to develop Sz are more likely to under-perform academically and are less likely to be in an age-

appropriate class as a result. The idea that cognitive symptoms are at the core of schizophrenia is lent further credence by the fact that cognitive symptomology remains the best predictor of long-term functional outcome (Lewis and Sweet 2009, Reichenberg and Davidson 2006). Cognitive pathology extends into deficits in socio-emotional processing. Deficits in attention, a distinctly neurocognitive domain, are strongly associated with the acquisition of social skills; indeed it is cognitive symptoms which correlate most strongly with functional impairment (Green 1996).

2.2 GENETIC AND ENVIRONMENTAL INFLUENCES

Sz is a highly heritable disorder, and while simple Mendelian genetics do not account for the transition to psychosis, recent evidence links a number of genetic loci to the disorder.

Genome–Wide Association Studies (GWAS) have identified a number of single nucleotide polymorphisms in genetic regions whose activity plays a role in glutamatergic circuitry (*NRGN*), synaptic function (*CACNA1C*), verbal ability (*ZNF804A*), neurodevelopment (*TCF4*), and immune response (*MHC*) (Consortium 2014, Owen et al 2010, Pocklington et al 2014). This lends support to the validity of the findings in that these systems are linked to the phenotypic expression of Sz. However, direct links between alterations to risk genes and the development or pathology of Sz have not been identified. It is important to recognize that, individually, identified risk alleles confer little to disease liability. Summing the effect of contributions from thousands of common, small effect alleles reveals a robust polygenic component to disease heritability. The emerging genetic picture involves the dual contribution from many, common small-effect allelic variants and more rare risk variants with much greater effect (Owen et al 2010). The interplay between the genetics and pathophysiology of Sz is

difficult to disentangle because target genes perform varied cellular functions and interact with a multitude of protein partners. As a result of complex heritability, broadly overlapping symptoms, and shared genetic risk loci, Sz is often comorbid with other diagnoses including affective, addiction, and anxiety disorders. Specifically, risk loci *CACNA1C* and *ZNF804A* achieve genome-wide significance in GWAS of Bipolar Disorder (BD). This fact, combined with evidence that polygenic scores of risk-alleles common in Sz are found in higher prevalence in BD than in controls, suggests a strong genetic overlap between the disorders (Owen et al 2010). It is clear that Sz is a complex trait. The polygenic allelic variation which underlies Sz also underlies non-clinical endophenotypes present in unaffected first degree relatives, and the common allelic variations apparent in Sz are found in individuals without any identifiable neurodevelopmental phenotype. The high genetic variability of Sz has led some to postulate that Sz is in truth a group of phenotypically related disorders that are etiopathologically distinct (Consortium 2014).

Data from twin cohorts produce two clear lessons about the heritability of Sz. The first is the degree of shared genetics predicts liability to Sz in relatives to those with the disorder; the second is that environmental effects play an enormous role in producing clinical pathology despite genetic vulnerability. As stated above, the global prevalence of Sz is ~1%; however, the incidence rate doubles in 3rd degree relatives, increases to as high as 6% in 2nd degree relatives, and increases further to between 6-17% in 1st degree relatives. Dyzogtic twins share an incidence rate of ~17% and monozygotic twins share an incidence rate ~50%. Meta-analysis of twin studies places the estimate of heritability of liability to Sz at ~81% (Lewis and Lieberman 2000, Sullivan et al 2003). Given that monozygotic twins are genetically identical, the fact they do not share absolute concordance for Sz reveals unique environmental effects play a significant

role in developing clinical pathology even when environmental influences greatly overlap (e.g. shared gestation, common upbringing). A number of environmental risk factors, clustered during early development, have been found to contribute to the prevalence of Sz including prenatal maternal infection, prenatal maternal stress, fetal hypoxia, and obstetric complications (Ellman and Cannon 2006). Other environmental risk factors have their effect during later maturational stages, including early childhood social isolation, heavy adolescent cannabis exposure, emigration to a region in which one is an ethnic or racial minority, and urban residency (Lewis and Lieberman 2000).

2.3 AUDITORY CORTEX AS MODEL CORTICAL SYSTEM

Many studies of the cortical pathology associated with Sz focus on areas responsible for executive function and memory. However, the auditory cortex is an especially important site for understanding the pathophysiology of Sz. While the pathogenesis of the disorder involves genetic factors and developmentally early insults, the first episode of psychosis rarely occurs before the onset of puberty. The maturation of the auditory cortex follows a parallel timeline and is not complete until an individual's third decade. This protracted maturational process may leave this region particularly vulnerable to the effect of environmental stressors, an idea which is supported by structural, cellular, and molecular alterations specific to this area in disease (Moyer et al 2015). As is discussed in further detail below, abnormalities in the auditory domain are tightly linked to schizophrenia pathology with serious implications for the individual's prognosis and abilities. For additional information on the role of the auditory cortex in disease, see section 3.1. The auditory cortex has added value as a model system in its conservation through species.

Prefrontal regions are uniquely developed in primate species, especially humans, which makes modelling the relationships between structural and molecular changes and alterations to behavior in animal models difficult to interpret.

3.0 LOSS OF MICROTUBULE ASSOCIATED PROTEIN 2 IMMUNOREACTIVITY LINKED TO DENDRITIC SPINE LOSS IN SCHIZOPHRENIA

3.1 INTRODUCTION

Individuals with schizophrenia (Sz) present with a number of functional deficits in the auditory domain. Patients exhibit impaired performance on pure tone discrimination tasks, an inability which does not depend on attention and thus implicates the auditory cortex itself (2000, Leitman et al 2010, Rabinowicz et al 2000). This functional deficit has consequences for social cognition in individuals with the disorder in that it makes prosody detection more difficult (Javitt 2009, Leitman et al 2006). In electrophysiological studies, Sz subjects display reduced amplitude on mismatch negativity(Javitt et al 2000, Naatanen and Kahkonen 2009, Umbricht et al 2003, Umbricht and Krljes 2005) (MMN), an event-related potential generated in the primary auditory cortex in response to stimuli deviant from preceding stimuli with respect to a particular feature (e.g. pitch, amplitude, duration)(Javitt et al 1994). Performance on tone discrimination tasks and MMN amplitude are correlated, and impairments on both are linked to severity of positive and negative symptoms (Hermens et al 2010, Javitt et al 2000, Rabinowicz et al 2000).

These functional and electrophysiological deficits are paralleled at the cortical level by progressive gray matter volume reduction in the superior temporal gyrus (STG) in Sz subjects and first-degree relatives at high-risk (McCarley et al 1999, Rajarethinam et al 2004) and

specifically in Heschl's gyrus which contains the primary auditory cortex (Hirayasu et al 2000, Kasai et al 2003, Rajarethinam et al 2004, Salisbury et al 2007, Takahashi et al 2009) (Brodmann area 41; BA41). Reductions in gray matter are found at (Rajarethinam et al 2004, Takahashi et al 2009), or prior to transition to, (Hirayasu et al 2000, Kasai et al 2003, Salisbury et al 2007) the first psychotic episode indicating initial gray matter loss cannot be attributed to the effects of treatment or illness duration. STG gray matter loss is selective for individuals with Sz in comparison to those diagnosed with bipolar disorder (Hirayasu et al 2000, Kasai et al 2003, Salisbury et al 2007).

Gray matter volume loss in the auditory cortex in Sz is not explained by underlying reductions in layer 3 pyramidal neuron number(Dorph-Petersen et al 2009), and more likely represents reductions in pyramidal neuron somal size and excitatory connections in this cortical region (Sweet et al 2004, Sweet et al 2009). We previously described a decrease in the density of spinophillin-immunoreactive puncta in deep layer 3 of the primary auditory cortex in Sz, representing reductions in pyramidal neuron spine density paralleling findings of a loss of spines per length of dendrite described in other cortical regions (Garey et al 1998, Glantz and Lewis 2000, Rosoklija et al 2000). Sz is also characterized by a reduction in the extent and complexity of the dendritic arbor in hippocampus and cingulate and frontal cortices (Black et al 2004, Broadbelt et al 2002, Glantz and Lewis 2000, Kalus et al 2000). However, the molecular mechanisms that contribute to these concurrent reductions in dendrites and spines in disease are currently unknown.

Microtubule associated protein 2 (MAP2) stands at the intersection of these phenomena. MAP2 is the most prevalent isoform of the dendritic MAPs, a family of cytoarchitectural proteins that includes the axonal homolog MAP tau (Dehmelt and Halpain 2005, Sanchez et al

2000). MAP2 is an important regulator of neuritic development and maintenance that acts by binding and nucleating the primary structural component of the dendritic cytoskeleton, microtubule (MT) monomers and subsequently stabilizing and spacing mature MT bundles in the dendrite.(Belanger et al 2002, Dehmelt and Halpain 2005, Farah and Leclerc 2008, Sanchez et al 2000, Teng et al 2001). MAP2 plays a similar role in supporting the actin cytoskeleton in spines, binding and nucleating filamentous actin (f-actin) to regulate spine morphology.(Selden and Pollard 1983) MAP2 is regulated by development and experience-dependent plasticity, with these processes tightly controlling MAP2 function by phosphorylation across its functional domains (Sanchez et al 2000). MAP2 immunoreactivity (MAP2-IR) is markedly reduced in a number of different cortical regions associated with Sz pathology including those regions where reduction of the dendritic arbor has been described (Arnold et al 1991, Jones et al 2002, Rioux et al 2004, Rosoklija et al 2005, Somenarain and Jones 2010) (e.g. cingulate and frontal cortices, hippocampal formation). However, MAP2 mRNA expression levels are unchanged in the disorder suggesting that Sz pathology impacts MAP2 protein and not its transcript (Law et al 2004).

In the present study, we investigated whether MAP2-IR is diminished in deep layer 3 of the primary auditory cortex of Sz subjects and its potential association with spine reduction, which we have previously observed in this layer (Sweet et al 2009). To address this question, we used multi-label quantitative fluorescence microscopy to measure the intensity of MAP2-IR, spine density, and spine number in 20 subjects with Sz and matched controls. We found that MAP2-IR was significantly decreased in individuals with Sz, with a subset of 60% of Sz subjects that exhibited MAP2-IR levels below the lowest level observed in controls. MAP2-IR was significantly associated with spine density and spine number, with reductions in spine density

and number restricted to the 60% of subjects with Sz with MAP2-IR below normal levels. These findings suggest that MAP2 is functionally compromised by disease pathology with implications for dendritic arbor and dendritic spine structural integrity.

3.2 MATERIALS AND METHODS

3.2.1 Human Subjects

For this study, we used tissue from two cohorts (**Table 1**) comprised of subjects diagnosed with schizophrenia or schizoaffective disorder (together referred to as Sz) and controls matched on the basis of sex, and as closely as possible for age, post-mortem interval (PMI), and handedness. Brain tissue was obtained during autopsies conducted at the Allegheny County Office of the Medical Examiner, after receiving consent from next-of-kin using a mechanism approved by the University of Pittsburgh Institutional Review Board and Committee for Oversight of Research Involving the Dead. An independent committee of experienced clinicians made consensus DSM-IV (Diagnostic and Statistical Manual of Mental Disorders, 4th ed.) diagnoses for each subject, using information obtained from clinical records and structured interviews with surviving relatives as previously described.(Glantz and Lewis 2000, Sweet et al 2009)

	Cohort 1	**Cohort 2**	**Total**			
	Control	**Sz**	**Control**	**Sz**	**Control**	**Sz**
n	**12**	**12**	**8**	**8**	**20**	**20**
Mean Age (SD)	**45.2(12.9)**	**47.3(13.4)**	**46.4(14.0)**	**46.5(12.4)**	**45.8(13.0)**	**46.9(13.4)**
Range	**19-65**	**27-71**	**24-62**	**25-62**	**19-65**	**25-71**
Sex (F/M)	**3/9**	**3/9**	**4/4**	**4/4**	**7/13**	**7/13**

Handedness (R/L/A/U/)	**11/1/0/0**	**6/2/1/3**	**8/0/0/0**	**5/3/0/0**	**19/1/0/0**	**11/5/1/3**
PMI (SD)	**18.1(6.5)**	**17.9(8.8)**	**13.7(6.5)**	**15.6(6.8)**	**16.4(6.7)**	**17.0(7.9)**
Storage Time , Months (SD)	**155.0(27.2)**	**145.5(29.8)**	**97.1(22.4)**	**92.8(14.0)**	**131.8(38.2)**	**124.4(35.9)**
Illness Duration, Years (SD)		**22.1(14.7)**		**22(13.3)**		**22.1(13.8)**
Range		**3-50**		**4-41**		**3-50**
Age at Onset (SD)		**25.2(7.7)**		**24.5(9.6)**		**24.9(8.3)**
Suicide, n(%)		**2(16.7%)**		**2(25.0%)**		**4(20.0%)**
Schizoaffective, n (%)		**4(33.3%)**		**2(25.0%)**		**6(30.0%)**
Alcohol/ Substance Abuse ATOD		**5(41.7%)**		**0(0%)**		**5(25.0%)**
Anticonvulsant ATOD, n(%)		**5(62.5%)**		**1(12.5%)**		**6(30.0%)**
Antidepressant ATOD, n(%)		**3(37.5%)**		**5(62.5%)**		**8(40.0%)**
Antipsychotic ATOD, n(%)		**11(91.7%)**		**6(75.0%)**		**17(85.0%)**
Benzodiazepine ATOD, n(%)		**1(8.3%)**		**3(37.5%)**		**4(20.0%)**
History of Cannabis Use, n(%)		**5(41.7%)**		**2(25.0%)**		**7(35.0%)**
Tobacco ATOD, n(%)	**4(33.3%)**	**8(66.7%)**	**3(37.5%)**	**6(75.0%)**	**7(35.0%)**	**14(70.0%)**

Table 1. Subject Characteristics. Each Sz subject in cohorts 1 and 2 was previously matched to a normal control subject based on sex, and as closely as possible for age and postmortem interval. There were no diagnostic group differences in age [$t(38) = -0.333$, $p = 0.741$] or postmortem interval [$t(38) = -0.272$, $p = 0.787$]. The distribution of handedness between diagnostic groups reached trend level ($\chi 2 = 8.800$, $p = 0.066$). Mean tissue storage time did not differ between diagnostic groups [cohort 1: $t(22) = 0.817$, $p = 0.423$; cohort 2: $t(14) = 0.461$, $p = 0.652$].

F, female; M, male; R, right-handed; L, left-handed; A, ambidextrous; U, unknown; PMI, postmortem interval; ATOD, at time of death.

3.2.2 Antipsychotic-exposed Monkey Cohort.

We also used a previously described monkey (*Macaca fascicularis*) cohort comprised of four animals chronically administered the antipsychotic haloperidol decanoate and age, sex, and

weight matched control animals (**Figure 1** top panels) (Akil et al 1999, Moyer et al 2012, Moyer et al 2013, Sweet et al 2009). Over a period of 9-12 months, macaques were intramuscularly administered the antipsychotic haloperidol decanoate every four weeks at a dose [mean (standard deviation)] of 16 (2.1) mg/kg which maintained trough serum levels at 4.3 (1.1) ng/ml. Similar concentrations have been associated with a therapeutic response in humans, (Volavka et al 1992) and resulted in extrapyramidal symptoms, which were effectively controlled in all treated animals with benztropine mesylate.

At the end of haloperidol exposure, all animals were euthanized by pentobarbital overdose; brains were removed and immersed in 4% paraformaldehyde following a 45 minute PMI. Primary auditory cortex was identified in sections from the STG using previously described cytoarchitectonic and immunohistochemical features (Sweet et al 2004). All protocols were approved by the University of Pittsburgh's Institutional Animal Care and Use Committee.

3.2.3 Human Tissue Processing

Brains from individuals in cohorts 1 and 2 were bisected and the left hemisphere was cut into 1-2 cm thick coronal blocks, which were then immersed in 4% paraformaldehyde in phosphate buffer for 48 hours, equilibrated in a series of graded sucrose solutions, and stored at -30˚C in an antifreeze solution.

The left superior temporal gyrus (STG) of each subject was dissected from fixed coronal blocks; reassembled in their *in vivo* orientation, and cut into 3mm thick slabs as previously described (Sweet et al 2005). Every other slab was selected, sectioned exhaustively, and adjacent sections stained for parvalbumin (PV), acetylcholinesterase (AChE), and Nissl substance for determination of the boundaries of the primary auditory cortex (Sweet et al 2005). For each

human and monkey subject, the borders of layers 2/3 and 3/4 were identified on the mapping sections to determine the total layer 3 area for each subject. A contour outline of the deepest one third of layer 3 was drawn in Stereo Investigator (**Figure 1,** MicroBrightField Inc., Colchester, Vermont). These contours were then aligned to the tissue sections used in the current study using pial surface fiduciaries.

For cohort 1, the primary auditory cortex was dissected from the unused slabs, and further subdivided into 3 mm wide blocks which were sectioned at 50 µm in an orientation perpendicular to the pial surface, and stored in antifreeze solution at -30˚C until selected for use in this study as described previously (Dorph-Petersen et al 2009, Moyer et al 2012, Moyer et al 2013). For cohort 2, 60 µm sections adjacent to the mapping sections were sampled systematic uniform random for assay (**Figure 1**).

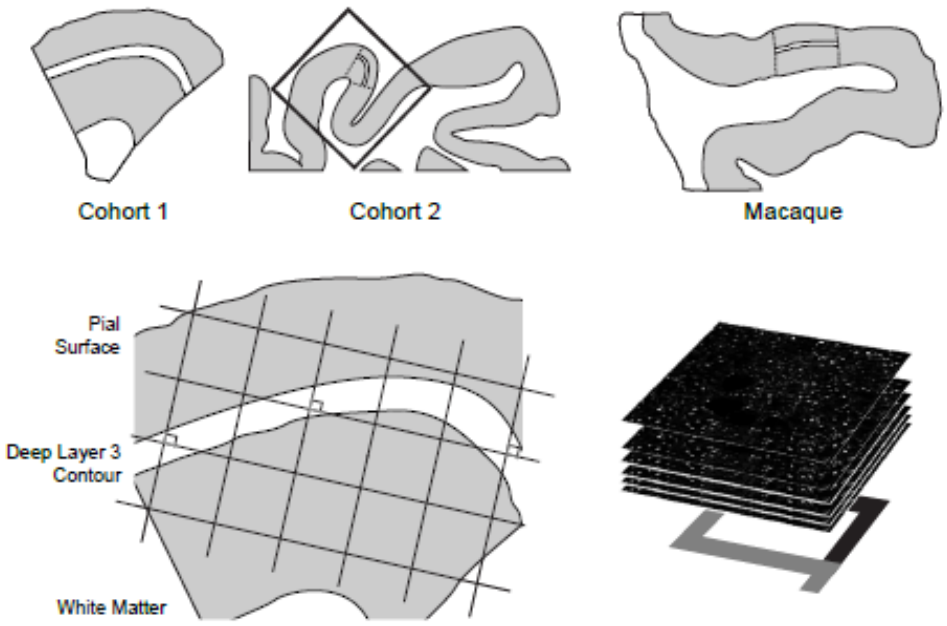

Figure 1. **Sampling of primary auditory cortex deep layer 3.**
(Top) Illustration of delineation of primary auditory cortex deep layer 3 on sections containing auditory cortex for human and antipsychotic exposed macaque cohorts. For each human and monkey subject, the borders of layers 2/3 and 3/4 were identified on

adjacent Nissl-stained sections to determine the total layer 3 area for each subject. A contour outline (shown in white) of the deepest one third of layer 3 was drawn in Stereo Investigator (MicroBrightField Inc., Colchester, Vermont). **(Bottom)** A sampling grid was created in Stereo Investigator to generate sampling sites for both human and nonhuman primate subjects. The grid was then randomly rotated, and a sampling site (shown as counting frames) was marked at every intersection between the grid and the deep layer 3 contour. At each sampling site, a 12.5-μm thick stack of 50 image planes, each separated by 0.25 μm, was collected using spinning disk confocal microscopy.

3.2.4 Immunohistochemistry

A single tissue section per subject was included in each run along with its matched pair for a total of 3-4 sections per subject from cohort 1 and 3 sections per subject from cohort 2. In order to visualize dendritic spines, we used two markers in combination: a polyclonal antibody directed against spinophilin and raised in rabbit (Millipore AB5669, Billerica, MA) at a dilution of 1:1500. The second was the f-actin binding mushroom toxin phalloidin (Invitrogen A12380, Carlsbad, CA) conjugated to Alexa Fluor® 568. Spinophilin is highly enriched in spine heads.(Allen et al 1997, Muly et al 2004) Phalloidin binds f-actin which is also highly enriched in dendritic spines (Capani et al 2001). These two labels show clear co-localization in structures resembling dendritic spines in human postmortem brain tissue (**Figure 2**) MAP2 was detected through the use of mouse monoclonal IgG antibody SMI-52 (Covance SMI-52R, Princeton, NJ) at a dilution of 1:500. SMI-52 has been shown to react with mammalian MAP2 both in culture and in fixed sections, robustly labeling the soma and dendritic arbor of neurons in human tissue (Anderson et al 1996). In immunoblot experiments, SMI-52 recognizes all isoforms of MAP2 (MAP2A, MAP2B, MAP2C) (Kaufmann et al 1997). Free-floating sections were pre-treated with 1%$NaBH_4$ to reduce auto-fluorescence and 0.3% Triton X in order to permeabilize the sections before being incubated for two hours at room temperature in blocking buffer comprised

of 20% normal human serum, 20% normal goat serum, 1% bovine serum albumin, 0.1% Lysine, 0.1% Glycine, and phosphate buffered saline (PBS). Following blocking, tissue was immediately placed in primary antibody buffer (5% normal human serum, 5% normal goat serum, 1% bovine serum albumin, 0.1% Lysine, 0.1% Glycine, PBS, and antibodies) overnight at 4˚C. Sections were rinsed in PBS then incubated in the same buffer, containing biotinylated goat anti-mouse (1:250; Invitrogen BA-9200), Alexa Fluor® 488 goat anti-rabbit (1:500; Invitrogen A11034), and Phalloidin- Alexa Fluor® 568 (3:200) at 4˚C for 24 hours. Tissue was again rinsed then incubated overnight in a 1:500 dilution of streptavidin Alexa Fluor® 647 (Invitrogen, S32357) at 4˚C. The tissue sections were subsequently mounted on gel-coated slides, rehydrated to ameliorate the effects of z-axis tissue shrinkage, and coverslipped using Vectashield hard-set H-1400 mounting medium (Vector Laboratories, Burlingame, CA). Sections from the antipsychotic- and control monkeys were processed together within immunohistochemistry runs using identical procedures.

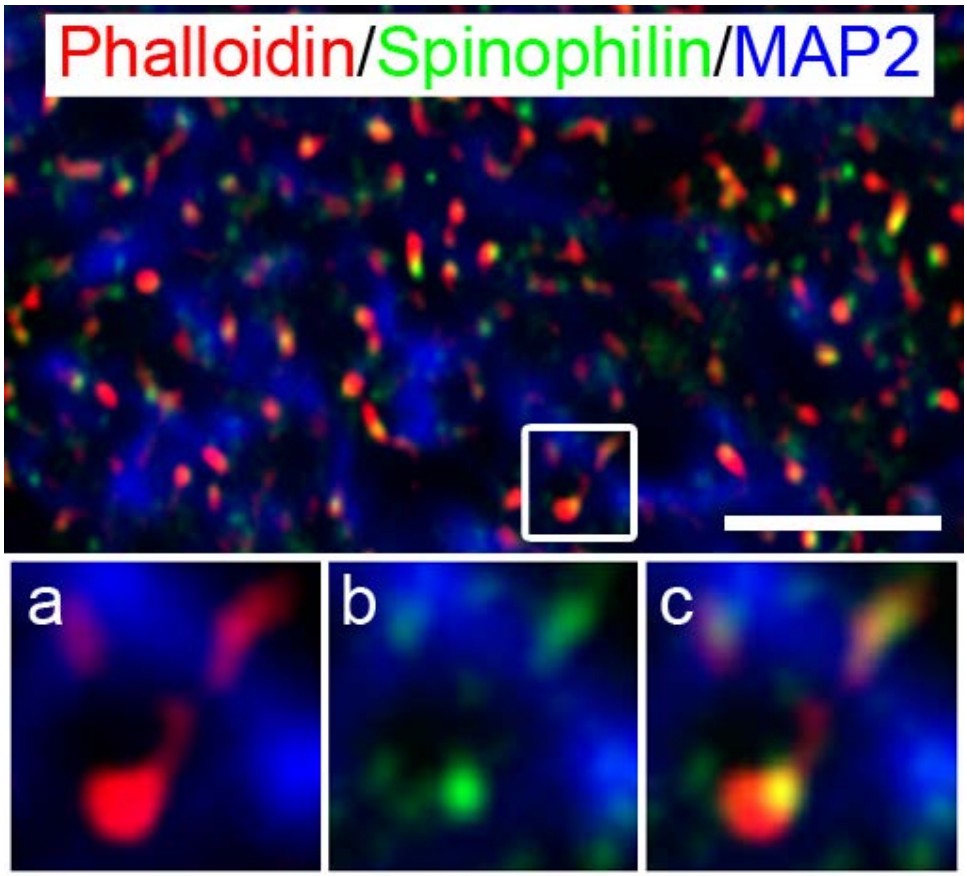

Figure 2. Phalloidin labeled and spinophilin-immunoreactive puncta in deep layer 3. (**Top**) Phalloidin labeled puncta (red) and spinophilin-IR puncta (green) co-localize throughout deep layer 3 of BA41 and are often organized along MAP2-IR processes (blue) suggesting spine structures along dendrites. Images below are a magnification of the inset in the top panel more closely revealing the relationship between phalloidin-labeled (a) and spinophilin-IR objects (b), and their co-localization in putative spine structures (c). Scale bar=5 µm.

3.2.5 Image Collection

Matched pairs from each cohort were imaged during the same session by an experimenter (JTN) blinded to diagnostic or antipsychotic exposure group All images were taken using a 1.42 numerical aperture (NA) 60X oil supercorrected objective mounted on an Olympus BX51Wl upright microscope (Olympus, Center Valley, PA) equipped with an Olympus DSU spinning disk, Hamamatsu Orca R2 camera (Hamamatsu, Bridgewater, NJ), MBF CX9000 front mounted digital camera (MicroBrightField Inc., Natick, MA), BioPrecision2 XYZ motorized stage with linear XYZ encoders (Ludl Electronic Products

Ltd., Hawthorne, NY), excitation and emission filter wheels (Ludl Electronic Products Ltd., Hawthorne, NY), Sedat Quad 89000 filter set (Chroma Technology Corp., Bellows Falls, VT), and a Lumen 220 metal halide lamp (Prior Scientific, Rockland, MA). The process of image collection was accomplished using Slidebook software version 5.027 (Intelligent Imaging Innovations, Denver, CO) and Stereo Investigator version 8 (MicroBrightField Inc., Natick, MA).

3.2.6 Image Processing

Images were processed using Slidebook software version 5.027 with keystrokes automated by Automation Anywhere software (Automation Anywhere, Inc. San Jose, CA). Camera background was subtracted from channels 488 and 568 prior to processing.

Single plane MAP2 images were masked using a threshold segmentation defined by the Ridler Calvard (RC) derived value in Slidebook. Underlying gray level values were extracted from the mask objects.

Image stacks were deconvolved using the AutoQuant adaptive blind deconvolution algorithm (MediaCybernetics, Rockville, MD). After deconvolution, edges were sharpened by taking the difference between images convolved at two standard deviations of the Gaussian distribution ($\sigma1=0.7$; $\sigma2=2.0$) as previously described, (Kirkwood et al 2013) then subjected to iterative intensity/morphological segmentation (Fish et al 2008). Spinophilin-IR and phalloidin puncta with intensity measures above the RC defined minimum threshold derived value in Slidebook were selected and contiguous pixels were defined as a 'mask object.' Spinophilin-IR and phalloidin mask objects with volumes between 0.1 and 0.8 µm3 and 0.04 and 1.5 µm3, respectively, were selected at each iteration. Due to lower spinophilin-IR intensity in cohort 2, it

was necessary to begin with a minimum threshold value at 1/3 the RC defined value. At each of 100 iterations, the threshold intensity was increased and the mask objects combined with those of the prior iteration.

3.2.7 Calculation of Spine Density and Number

While both spinophilin-IR and phalloidin binding are strongly localized to spines, each has some off target label (Capani et al 2001, Muly et al 2004) Therefore, identification of putative dendritic spines required co-localization of spinophilin-IR and phalloidin label **(Figure 2)**, operationalized as phalloidin mask objects that overlapped (≥ 1 voxel) with a spinophilin-IR mask object Spine density (Nv) and number (N) in cohort 1 was calculated as previously described with minor modification: (Moyer et al 2012, Moyer et al 2013)

$$N_v := \frac{\bar{t}_{wQ^-}}{h} \cdot \frac{\sum(Q_i^- \cdot w_i)}{BA \cdot a \cdot \sum(P_i \cdot w_i)}$$

Where a is the area of the counting frames, Q_i^- is the count of dendritic spines within the *i*th block, P_i is the count of the associated points hitting the region of interest in the *i*th block, *h*= disector height, *BA* is the cryostat block advance (50 µm for cohort 1 and 60 µm for cohort 2, $\bar{t}_{wQ^-}$ is the block-and-number-weighted mean section thickness calculated using this formula:

(2)

$$\bar{t}_{wQ^-} := \frac{\Sigma(t_j \cdot q_j^- \cdot w_i)}{\Sigma(q_j^- \cdot w_i)}$$

where t_j is the local section thickness measured centrally in the *j*th sampling frame and q_j^- is the corresponding count of dendritic spines in the *j*th frame. w_i is the block weight—i.e. either 1 or 1/3. The number of spines was estimated as the product of previously determined deep layer 3 volumes in these subjects (Dorph-Petersen et al 2009, Moyer et al 2012, Moyer et al 2013) and the N_v calculated in the above equation, represented here:

(3)

$$N := N_v \cdot V_{\text{deep layer 3}}$$

Because for cohort 2, sections adjacent to the mapping sections were sampled, calculation of N_v and N were as above but omitting the block weighting (Dorph-Petersen and Lewis 2011).

Phalloidin mask objects overlapping spinophilin mask objects were counted automatically by determining whether the centroid of each automatically detected object was inside the disector. This corresponds to the so-called "associated point rule" (Baddeley 2005), which is an unbiased alternative to the unbiased counting frame (Gundersen 1977). Guard zones of 10 pixels were applied around all edges in the X and Y dimensions of each stack, and a guard zone of 4 Z planes was provided starting at the top of the tissue below the coverglass. The resulting disectors were 492 x 492 pixels in X and Y dimensions, and 24 Z planes (cohort 1) or 4 Z planes (cohort 2). These Z ranges were selected based on evidence from calibration plots that puncta

counts and intensities were uniform across these Z axis depths. It should be noted that the relatively low disector height (1.0 µm in Cohort 2) could be implemented robustly because we used confocal microscopy allowing for a high number of thin focal planes, because of our use of deconvolution with full thickness reconstructions and determination of centroids; and because we performed a careful analysis of the distribution of the puncta along the Z axis. We determined the position of the disector and corresponding guard zones *post hoc* ensuring that puncta were only sampled in the zone with uniform bouton counts. Such sampling was also possible due to the high number of automatically detected puncta per subject. Thus, while a disector height of only 1.0 µm should be avoided in a standard brightfield microscopy study with manual counts, we were able to robustly implement such a disector in the current study.

3.2.8 Statistical Models

3.2.8.1 Human Tissue Study

For each subject in the human tissue study, the intensity of MAP2-IR was first log transformed to more normally distribute MAP2-IR data. To assess the diagnostic effect in log MAP2-IR, spine density, spine number and deep layer 3 volume, two analysis of covariance (ANCOVA) models were used. Because we pair subjects within each cohort on age, sex, and postmortem interval, the primary model included diagnosis, cohort (which in this case includes effects of assay run and imaging run because the cohorts were studied sequentially), pair nested within cohort as blocking factors and tissue storage time (which is not a pairing variable, but may affect assay fidelity) as a covariate. To then assess the robustness of results, a secondary model was

used with diagnosis, cohort, and tissue storage time as covariates, and in place of subject pairings, we instead enter as covariates the pairing variables: age, sex, and postmortem interval.

In order to examine the confound effect of each of the following factors: sex (F/M), manner of death (suicide), diagnostic variation (schizoaffective disorder (Y/N), age of onset, duration of disease)), antipsychotic use (Y/N), anticonvulsant use (Y/N), benzodiazepine use (Y/N), non-diagnosis related drug treatment (Y/N), and substance abuse/dependence at time of death [alcohol (Y/N), tobacco (Y/N), cannabis history (Y/N), non-specified (Y/N)], the pairwise percent difference in each of the four variables was analyzed. If the confound variable was dichotomous, a two sample t test was used. If the confound variable was continuous, a simple linear regression analysis was used. The percent difference in log MAP2-IR within a pair is calculated as:

$$\frac{(\log(\text{MAP2 intensity}) \text{ in Control} - \log(\text{MAP2 intensity}))}{\log(\text{MAP2 intensity}) \text{ in Control}} X\ 100\%.$$

The pairwise percent differences for other variables were calculated similarly.

The relationship between log MAP2-IR and spine density was determined by two methods: Pearson's correlation coefficient and alternatively optimized Kendall's tau. In order to examine the relationship between log MAP2-IR and spine density, both variables were dichotomized by choosing cutoff points. A 2 by 2 contingency table was calculated for each chosen set of cutoff points. Kendall's tau was used as the measure of association of the contingency table. An optimizing search was used to find the cutoff points for each of log(MAP2-IR) and spine density so that Kendall's tau was maximized. The asymptotic p-value was obtained for the Kendall's tau to test if it is different from 0.

Diagnostic effect in spine density and spine numbers were examined within of the MAP2 Low and MAP2 Normal subgroups using the same primary and secondary models used on the entire 20 pairs of subjects.

The analyses for diagnosis effect and confound effect were implemented in SAS PROC GLM with alpha 0.05; Kendall's tau was obtained in SAS PROC FREQ, and the Pearson correlation coefficient was obtained in SAS PROC CORR.

3.2.8.2 Monkey Tissue Study

For each observation in the monkey tissue study, log MAP2-IR was taken before analysis so that MAP2 intensity was more normally distributed. Haloperidol treatment effect was examined with two mixed effect models: a primary model with treatment, assay and pair as fixed effect and monkey as a normal random effect to account for the repeated measures within one monkey; the secondary model was the same as the primary model except that pair was not included in the model. The analyses for the monkey tissue study were implemented in SAS PROC MIXED with alpha=0.05.

3.3 RESULTS

3.3.1 MAP2 Immunoreactivity

MAP2-IR was significantly reduced in Sz subjects compared to their matched control pairs (**Figure 3**) [primary model: $F(1,18)=18.32$; p=0.001 and secondary model: $F(1,33)=13.88$;

p=0.001]. There was a 70.0% reduction in log MAP2-IR in Sz subjects relative to controls based on the primary model. The mean log MAP2-IR (SE) for control and Sz subjects was 3.068 (0.085) for controls and 2.545 (0.092) for Sz subjects.

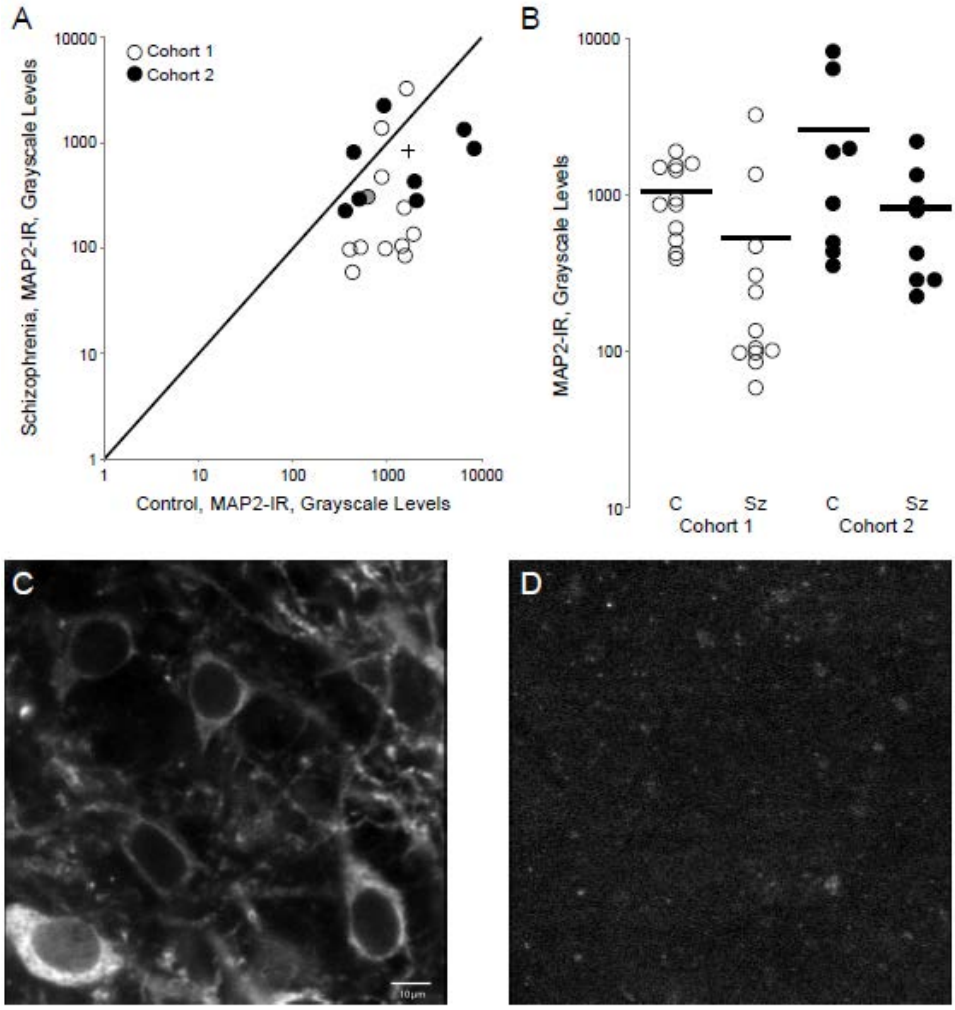

Figure 3. MAP2-IR is significantly reduced in Sz primary auditory cortex.
(A) MAP2-IR in subject pairs from cohort 1 and cohort 2. The unity line represents schizophrenia=control values; points beneath the line represent pairs in which schizophrenia<control; points above the line represent schizophrenia>control. The plus indicates the group mean. **(B)** MAP2-IR for control and schizophrenia subjects in cohort 1 and cohort 2. Bars represent mean IR for each group. (C-D) Representative micrographs of MAP2-IR taken from a control subject (left) and schizophrenia subject (right); scale bar= 10 µm. (cohort 1, pair 8, filled circle in A).

3.3.2 Primary Auditory Cortex Deep Layer 3 Neuron Number in Cohort 1 Subjects

We previously reported that pyramidal neuron number did not differ between control subjects and schizophrenia subjects in individuals from cohort 1 (Dorph-Petersen et al 2009). Mean layer 3 pyramidal neuron number for control subjects was 3.38×10^6 and 4.11×10^6 for schizophrenia subjects, a non-significant difference ($F_{1,10}=1.25$; $p=0.29$) The relationship between MAP2-IR and pyramidal neuron number is show in **Figure 4**). This finding confirms that MAP2-IR loss is not a result of pyramidal neuron loss.

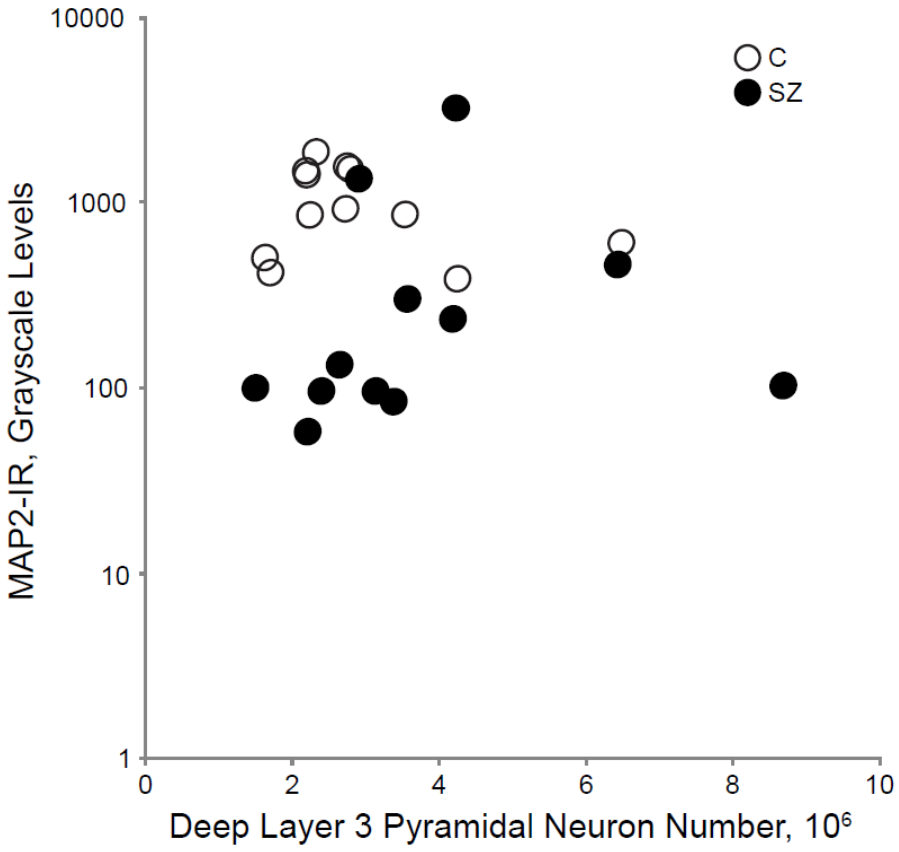

Figure 4. No loss of pyramidal neuron number in primary auditory cortex.
MAP2-IR plotted as a function of deep layer pyramidal neuron number in primary auditory cortex in control subjects (open circles) and schizophrenia subjects (filled circles) from cohort 1. For all subjects, $r^2=0.013$; the corresponding values for control,

r^2=0.0828 and schizophrenia subjects, r^2=0.0047. None of the correlations were significant.

3.3.3 MAP2 Peptide Amount in Primary Auditory Cortex Deep Layer 3

MAP2-IR loss could reflect a loss of protein, or a reduction in the ability to bind to its epitope. To determine if MAP2-IR loss is driven by a loss of protein, total protein was extracted from gray matter homogenates obtained from Heschl's gyrus containing the primary auditory cortex as previously described (Deo et al 2012). Five MAP2 peptides representing sequences along the length of MAP2 protein (**Figure 5, Top**) were quantified using liquid chromatography-mass spectrometry with selected reaction monitoring and quantification via a stable isotope labeled mouse brain standard as previously described (MacDonald et al 2012). MAP2 peptides were quantified in 5 pairs of subjects from the present study in whom the schizophrenia (Sz) subject exhibited MAP2-IR values below the lowest control value observed in the entire cohort, deemed MAP2-IR Low We found no significant differences in MAP2 peptide levels, despite substantial reductions in MAP2-IR in these same subject pairs (**Figure 5, Bottom**).

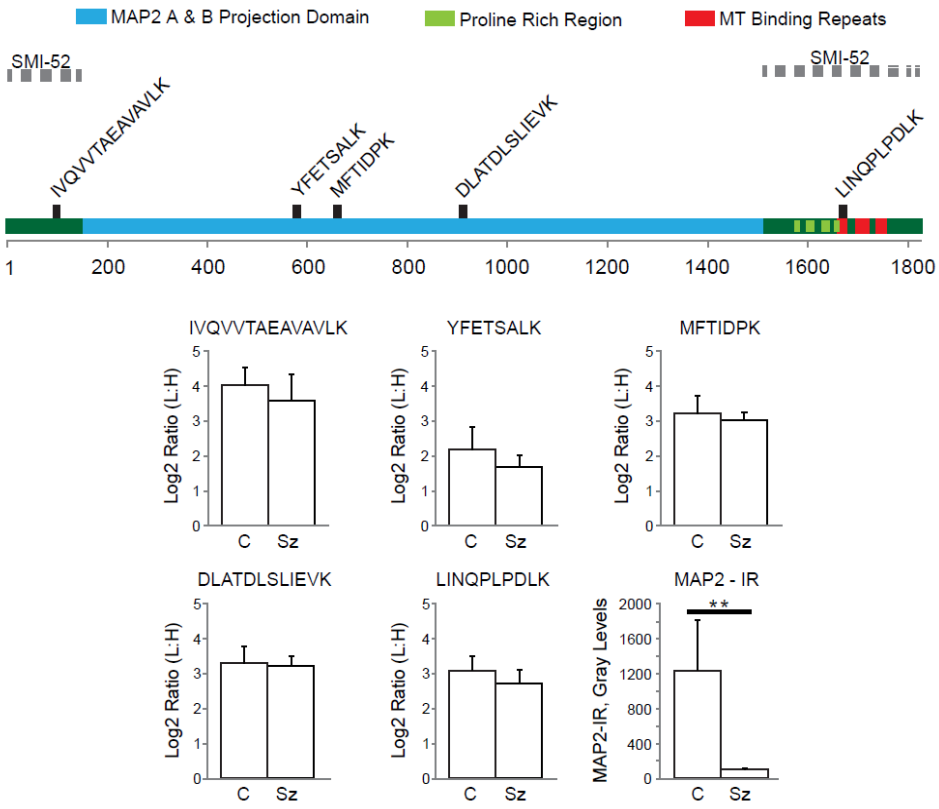

Figure 5. MAP2 peptide levels are unchanged in MAP2-IR Low Sz subjects.
(**Top**) Schematic of MAP2 protein isoforms. Dark green shows amino acids included in isoform MAP2C, whereas MAP2A and MAP2B also include the projection domain shown in blue. The locations of other functional domains along the length of MAP2 (numbering indicates amino acids) are as indicated. Dashed gray lines indicate the potential regions within MAP2 to which antibody used in this study (SMI-52, Covance) binds. The peptide sequences used for subsequent quantification are shown in their respective locations within the MAP2 protein. (**Bottom**) Mean ratios of MAP2 peptides in five MAP2-IR Low pairs (control, C; schizophrenia, Sz). Mean MAP2-IR for the same 5 pairs is shown in last panel. **, $p<0.01$. Error bars are SEM.

3.3.4 Influence of Post-Mortem Interval on MAP2 Immunoreactivity

We found no significant effect of post-mortem interval (PMI) in log MAP2-IR based on our secondary model in which the term pair is replaced by age, PMI, and sex ($F_{(1,33)}$=0.06, p=0.81; **Figure 6**).

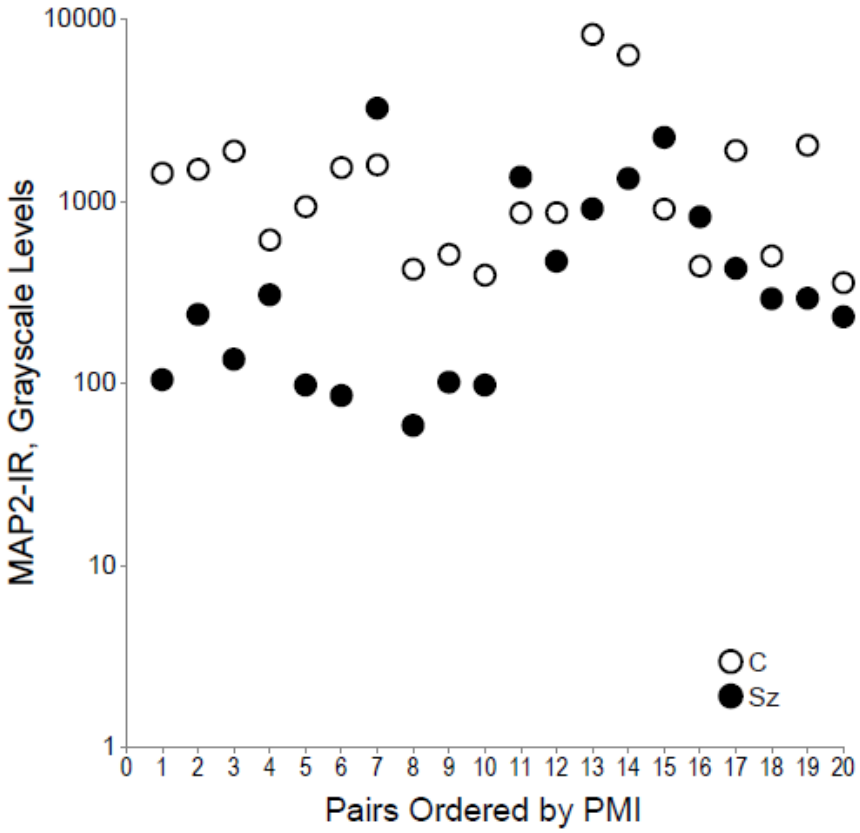

Figure 6. MAP2-IR is unaffected by PMI.
We found no significant effect of PMI on MAP2-IR. MAP2-IR is shown for each pair in order (from left to right) of ascending PMI of the Sz subjects. Control subjects open circles; schizophrenia subjects, filled circles.

3.3.5 Spine Density and Number

Mean spine density was significantly reduced in Sz subjects compared to matched controls [**Figure 7A**; primary model: $F(1,18)=6.17$; p=0.023 and secondary model: $F(1,33)=8.83$; p=0.005]. Mean spine density for control subjects [0.0333 µm -3 (0.0018)] and Sz subjects [0.0269 µm3 (0.0020)] revealed a 19.22% reduction in spine density.

The reduction in spine density in Sz subjects was paralleled by an accompanying reduction in mean spine number [**Figure 7B**; primary $F(1,18)= 4.13$, p=0.057 and secondary

F(1,33)=4.46, p=0.042]. The mean spine number (reported in billions) for control and Sz subjects were 1.30(0.083) and 1.06(0.009) respectively; a 18.79% reduction in spine number across diagnosis. In the secondary model, the effect of cohort was significant [*F*(1,33)= 6.33, p=0.017] but the diagnosis by cohort interaction was not significant.

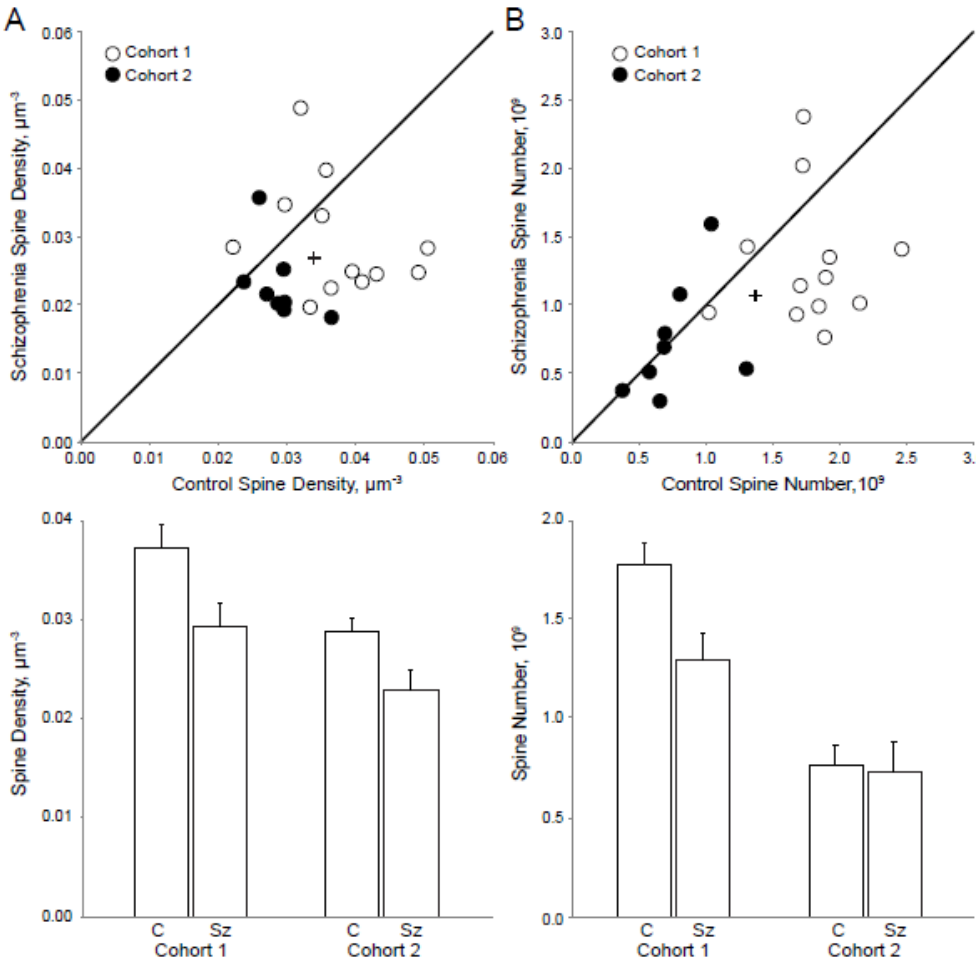

Figure 7. Spine number/density reduced in Sz primary auditory cortex.
(A) (Top) Mean spine density in deep layer 3 of primary auditory cortex in pairs from cohort 1 and 2. The unity line represents schizophrenia=control values; points beneath the line represent pairs in which schizophrenia<control; points above the line represent schizophrenia>control. The plus indicates the value of the group mean. **(Bottom)** Mean spine density for control (C) and schizophrenia (Sz) subjects in cohort 1 and cohort 2. Error bars are ± SEM. **(B) (Top)** Spine number in deep layer 3 of primary auditory cortex in subject pairs. The unity line and plus symbol represent the same relationships as described above. **(Bottom)** Mean spine number for control (C) and schizophrenia (Sz) subjects. Error bars are ± SEM.

3.3.6 Association with Clinical Factors

We examined the effect of a number of clinical factors (e.g. sex, manner of death, diagnostic variation, drug exposure, and substance abuse/dependence at time of death) on pairwise percent difference in MAP2-IR, spine density, and spine number. No significant associations were detected.

3.3.7 Correlation between MAP2-Immunoreactivity and Dendritic Spine Density and Number

There was a significant linear correlation between MAP2-IR and spine density (r2=0.433, p=0.005) but not between MAP2-IR and spine number (r2=0.162, p=0.32). However, the optimized Kendall's tau approach indicated that MAP2-IR and spine density were significantly related to each other based on the highest Kendall's tau obtained (τ=0.562, z=3.08, p=0.002), as were MAP2-IR and spine number (τ=0.5295, Z=4.48, $p<0.001$).

Twelve Sz subjects (60%) exhibited MAP2-IR values below the lowest control value, deemed MAP2-IR Low. MAP2-IR Low subjects had significant reductions, relative to their matched controls, in spine density [**Figure 8**; primary: F(1,10)=15.970, p=0.003 and secondary: F(1,17)=16.9, p=0.001] and spine number [**Figure 8;** primary: F(1,10)=12.06, p=0.006 and secondary: F(1,17)=12.01,p=0.003]. MAP2-IR Normal Sz subjects did not differ from their matched controls in either spine density [**Figure 8;** primary: F(1,6)=0.040, p=0.851 and secondary: F(1,9)=0.060, p=0.817] or spine number [**Figure 8;** primary: F(1,6)=0.12,p=0.74 and secondary: F(1,9)=0.15,p=0.708].

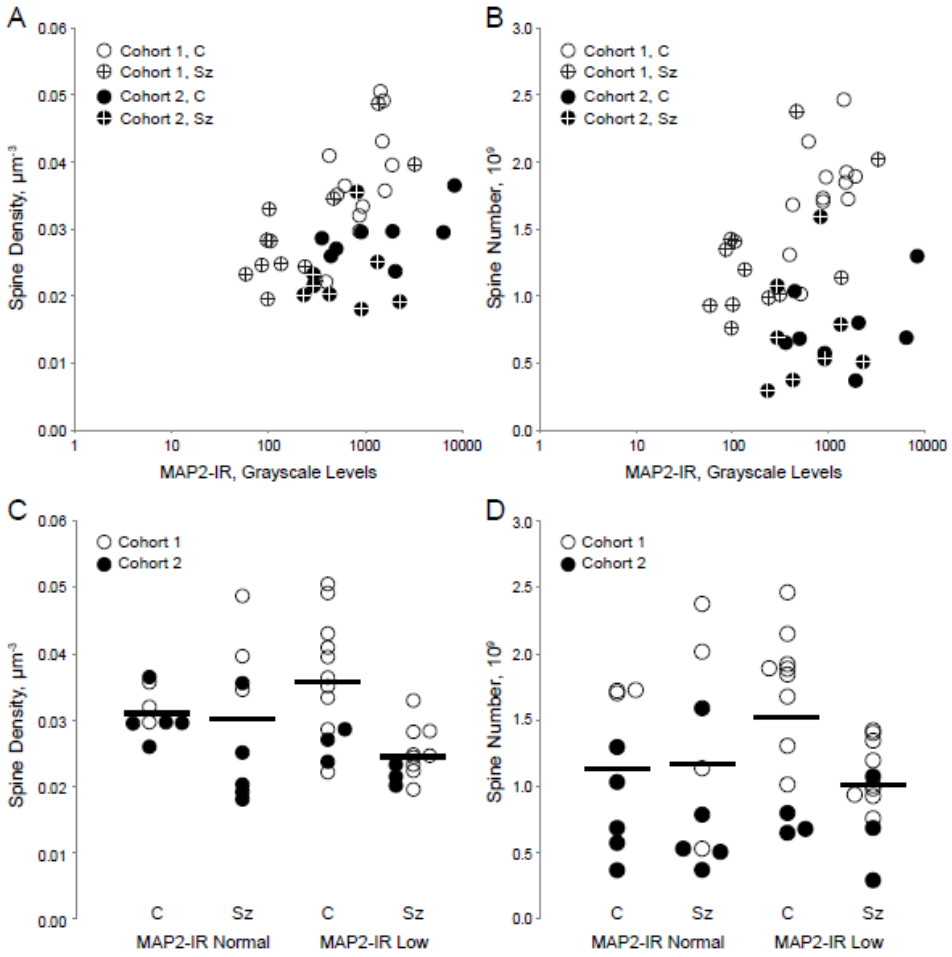

Figure 8. Relationship of MAP2-IR to dendritic spine number/ density.
(A) Mean spine density plotted as a function of MAP2-IR for control subjects (open) and schizophrenia subjects (crossed) in cohort 1 (unfilled) and cohort 2 (filled). **(B)** Spine number as a function of MAP2-IR for control subjects (open symbols) and schizophrenia subjects (crossed symbols) in cohort 1 (unfilled) and cohort 2 (filled). **(C)** Spine density for control (C) and schizophrenia (Sz) subjects in pairs in which the Sz subject MAP2-IR was above (MAP2-IR Normal) or below (MAP2-IR Low) the minimum MAP2-IR observed in control subjects. Bars represent mean values for each group. **(D)** Spine number for control (C) and schizophrenia (Sz) subjects in pairs in which the Sz subject MAP2-IR was above (MAP2-IR Normal) or below (MAP2-IR Low) the minimum MAP2-IR observed in control subjects. Bars represent mean values for each group.

3.3.8 Antipsychotic Exposed Monkeys

We found no significant effect of chronic haloperidol exposure on MAP2-IR. [**Figure 9;** primary $F(1,2.77)=0.54$ $p=0.52$ and secondary $F(1,5.76)=0.15$ $p=0.71$]. We previously reported no significant effect of haloperidol exposure on spine density in this group of animals. (Sweet et al 2009)

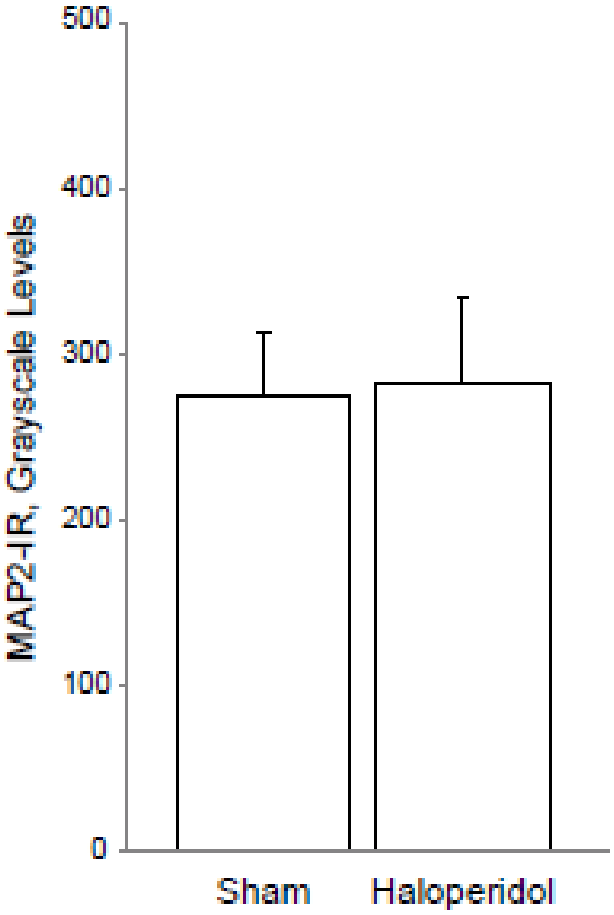

Figure 9. Mean MAP2 intensity is unchanged in haloperidol exposed macaques.
Chronic antipsychotic exposure did not alter MAP2-IR in adult male macaques. Error bars are ± SEM.

3.4 DISCUSSION

We hypothesized MAP2-IR is reduced in BA41 of individuals with Sz. Using quantitative fluorescence confocal microscopy, we examined alterations in MAP2-IR intensity in BA41 deep layer 3 and examined the relationship between MAP2-IR and dendritic spine markers within the same region. We found that MAP2-IR intensity was significantly reduced in Sz subjects in comparison to matched control subjects. Dendritic spine density and number were also reduced and were associated with MAP2-IR intensity. Twelve (60%) Sz subjects exhibited MAP2-IR intensity levels lower than the lowest control value. In this subset, deemed MAP2-IR Low, there were significant reductions in spine density and spine number while there were no significant reductions in spine density and number in MAP2-IR Normal subjects. Our findings are the first to show a change in MAP2-IR within the auditory cortex of individuals with Sz, and to relate MAP2-IR to dendritic spine alterations.

3.4.1 Schizophrenia Associated MAP2-IR Changes

We found a significant reduction in MAP2-IR in BA41 deep layer 3. Although the immunoreactive intensity and subcellular location of MAP2 are sensitive to the effects of increasing PMI (**Figure 6**), (Schwab et al 1994) it is unlikely that our finding can be attributed to the effects of PMI or effects of age, sex, and storage time. Our subject pairs were well matched for these variables, mitigating their influence. Moreover, we saw no significant association of any of the aforementioned variables with MAP2-IR within our statistical models, and no significant interactions between them and diagnosis. Similarly, none of the prior studies of MAP2-IR in Sz found significant effects of age, sex, or PMI. (Arnold et al 1991, Jones et al

2002, Rioux et al 2004, Rosoklija et al 2005, Somenarain and Jones 2010) Neither we, nor Rosoklija et al. (Rosoklija et al 2005) found a significant effect of antipsychotic treatment. Finally, we examined whether reduced MAP2-IR results from long term antipsychotic exposure in an animal model, and found no effect on MAP2-IR.

Many previous reports have documented reductions in MAP2-IR in other cortical regions linked to Sz pathology.(Arnold et al 1991, Jones et al 2002, Rioux et al 2004, Rosoklija et al 2005, Somenarain and Jones 2010) The drastic nature of the change in IR lends itself to macroscopic observation, which has allowed some groups to qualitatively assess regional IR. Within their cohort, Arnold et al.(Arnold et al 1991) found a qualitative loss of MAP2-IR in the subiculum and entorhinal cortex of 83% and 66% of their Sz subjects respectively; similar to our observation of marked MAP2-IR loss in the auditory cortex in 60% of our Sz subjects. Rosoklija et al. (Rosoklija et al 2005) reported qualitatively low or absent MAP2-IR in the subiculum of 20% of Sz subjects within their cohort but no overall change in IR in comparison to controls within the other hippocampal subfields. In order to quantify this change, others utilized optical density measurements or area fraction analysis.(Jones et al 2002, Somenarain and Jones 2010) As measured by Jones et al.(Jones et al 2002), MAP2-IR area fraction was decreased by 45% in layer 5 of frontal cortex (BA9) and 40% in layer 3 of BA9, 44% in layer 5 of cingulate cortex (BA32), and 32% in layer 3 of BA32 in Sz subjects compared to controls. Somenarain (Somenarain and Jones 2010) found a similar result in BA9 area fraction: a 38% reduction in layer 5 and a 39% reduction in layer 3.

Others (Jones et al 2002, Somenarain and Jones 2010) investigated the relationship between MAP2-IR reductions and neuron loss finding no differences in cell density in areas that showed a disease-specific reduction in MAP2-IR. Similarly, in a previous report,(Dorph-

Petersen et al 2009) the pyramidal neuron number in the twelve pairs that comprise cohort 1 in the present work was determined to be unchanged in BA41 layer 3 (**Figure 4**). Arnold et al. (Arnold et al 1991) found no neuron loss or accompanying increase in markers of neurodegeneration (e.g. gliosis, neurofibrillary tangles) in subjects with a decrease in MAP2-IR, while Rosoklija et al.(Rosoklija et al 2005)found no increase in gliosis as assessed by glial fibrillary acidic protein IR. It is clear from these data that neuron loss does not account for reductions in MAP2-IR. Further, using liquid chromatography-mass spectrometry, we have shown that MAP2-IR loss is not a result of MAP2 protein loss (**S2**.).

The large number of positive studies, despite the different regions, antibodies, and approach to quantification, in conjunction with evidence that reduced MAP2-IR does not result from common confounds such as PMI, age, and antipsychotic treatment, together lend confidence to the conclusion that reduced MAP2-IR represents a disease-associated alteration present across cortical regions in a large proportion of subjects with Sz. This interpretation raises important questions: what does the decrease in MAP2-IR indicate in terms of molecular changes to MAP2, and what consequences might MAP2-IR loss have for neuronal function in Sz?

3.4.2 Molecular Changes in MAP2 Leading to MAP2-IR Loss

MAP2, like its axonal homolog MAP tau, is tightly regulated by a strict balance of phosphorylation; extremes in either direction lead to decreased MT binding, nucleation, assembly, and stabilization. (Brugg and Matus 1991, Murthy and Flavin 1983, Sanchez et al 2000, Tsuyama et al 1986) It is important to note, that even at intermediate, endogenous levels of phosphate load, site-specific phosphorylation is more important than total phosphate amount in regulating MAP2-MT interaction.(Ainsztein and Purich 1994, Brugg and Matus 1991) MAP2 is

comprised of four functional domains tasked with different roles: 1) the n-terminal domain, which binds the RII subunit of cAMP-dependent protein kinase (PKA) 2) the 1372 amino acid (aa) projection domain found only in high molecular weight isoforms of MAP2 (i.e. MAP2A and MAP2B) that regulates the spacing of MT bundles (Belanger et al 2002) 3) the regulatory proline rich region, and; 4) the microtubule binding domain (MTBD) responsible for binding to MT's and actin. (Sanchez et al 2000) A number of protein kinases and phosphatases interact with sites within each region resulting in diverse functional consequences. To illustrate, PKA incorporates phosphate groups at sites primarily within the n-terminal and projection domains, thereby disrupting MAP2-MT binding and MT nucleation. (Itoh et al 1997) Similarly, Cdc2 kinase, which phosphorylates the MTBD, also disrupts MAP2-MT binding and MT nucleation, but additionally disrupts MT stabilization.(Itoh et al 1997) Even within functional domains, site-directed kinases can produce highly specific effects.(Ainsztein and Purich 1994) Although MAP2 is a natively unfolded protein, it can adopt complex folded conformations; a process that is sensitive to divalent cation concentration and depends on the C-terminal MTBD.(Ainsztein and Purich 1994, Di Noto et al 1999, Wille et al 1992) While not firmly established, it has been proposed that this process could potentially be a result of the high abundance of proline residues within the 156 aa adjacent to the MTBD. (Farah and Leclerc 2008, Sanchez et al 2000) Proline has the ability to exist in cis- and trans- isomers based on phosphorylation state and therefore may underlie MAP2's previously observed ability to fold upon itself. (Wille et al 1992) Phosphorylation-dependent folding has been previously demonstrated in MAP tau models of disease. (Jeganathan et al 2008) Thus, the reduction of MAP2-IR in our Sz subjects could indicate disease-associated alterations in MAP2 phosphorylation which, via changes in binding to MT targets or in folding, prevents the antibody from reaching its binding site.

It should be noted that other possibilities exist to explain MAP2-IR loss. Rather than a change in MAP2 protein, the phenomenon could represent a change in the network of proteins that bind MAP2. Outside of its role in the cytoskeleton, MAP2 serves as a receptor for the neurosteroids pregnenolone (PREG) and dehydroepiandrosterone (DHEA), an interaction which impacts dendritic stability, changes MAP2 phosphorylation state, and influences MAP2 immunostaining. (Fontaine-Lenoir et al 2006, Murakami et al 2000) Recent studies have identified changes in serum levels of both of these neurosteroids in patients with first-episode psychosis and linked this phenomenon to symptom severity.(Ritsner 2011) MAP2 also serves as an anchoring protein linking PKA to class C L-type Ca2+ channels,(Davare et al 1999) a class of voltage gated Ca2+ channels that have been linked to Sz by genomic studies.(He et al 2014) Genetic studies have also identified genes in the immediate early gene activity-regulated cytoskeleton-associated gene, *Arc*, pathway as linked to schizophrenia(Fromer et al 2014, Purcell et al 2014). *Arc* is locally expressed in the dendritic arbor in response to neuronal activity, and it has been demonstrated both *in vivo* and *in vitro* that up-regulation of *Arc* reduces MAP2-IR independent of MAP2 protein loss.(Fujimoto et al 2004) Dysregulation of NMDA receptor activity also changes the subcellular location of the MT plus end capping protein EB3, causing it to bind MAP2 at the MTBD.(Kapitein et al 2011) Disease state could potentially alter any of these partners, increasing their MAP2 binding and thus obscuring the antibody epitope. In support of such an interpretation, Cotter et al.(Cotter et al 2000) found increased MAP2-IR dendritic length in subiculum and hippocampus of subjects with schizophrenia using an antigen retrieval method that disrupts non-covalent protein binding (and/or MAP2 folding), potentially representing a greater unmasking of MAP2-IR sites in schizophrenia subjects.

3.4.3 Potential Consequences of MAP2-IR Loss for Neuronal Function in Schizophrenia

A primary role of MAP2 is stabilizing mature MT bundles in the dendrite. (Belanger et al 2002, Dehmelt and Halpain 2004, Farah and Leclerc 2008, Sanchez et al 2000, Teng et al 2001) Recent evidence has elucidated effects of MTs on dendritic spine morphology, finding that dynamic MTs enter developing and mature dendritic spines in response to synaptic activity. (Gu et al 2008, Hu et al 2008, Jaworski et al 2009) This entry leads to a transition from immature filopodia to mature mushroom head structure in developing spines. (Hu et al 2008, Jaworski et al 2009) Similarly, MT entry into spines has been demonstrated to be protective against spine reduction induced by long term depression, a process in which MAP2 participates. The link between spine structural plasticity and MAP2 is further supported by findings that inhibition of MT polymerization leads to a loss of mature spine structure, prevents long-term potentiation, and ultimately, ends in a drastic loss of spines themselves.(Gu et al 2008, Hu et al 2008, Jaworski et al 2009)

We therefore hypothesized that MAP2-IR reductions would be associated with dendritic spine loss in Sz. Our hypothesis was supported by our finding that the reduction in dendritic spines in Sz subjects was restricted to those with substantial reductions in MAP2-IR. Our finding replicated and extended our prior observation that dendritic spine density is significantly lower in deep layer 3 of primary auditory cortex in individuals with Sz. (Sweet et al 2009) The current observation was made in a non-overlapping cohort of subjects. Furthermore, by using stereologic methods to provide an estimation of spine number, we also showed that the reported loss in spine density reflects a loss of spines themselves as opposed to an expansion in surrounding tissue volume. This finding parallels Golgi-impregnation studies which have documented a Sz-

associated loss of layer 3 spine structures per unit of dendrite length in dorsolateral prefrontal cortex(Garey et al 1998, Glantz and Lewis 2000) and subiculum.(Rosoklija et al 2000) In addition, the loss of dendritic spines, in the absence of a change in neuron number, can be seen as congruent with earlier hypotheses of reduced neuropil in schizophrenia(Selemon and Goldman-Rakic 1999). In contrast, the reduced detectability of dendrites due to lower MAP2-IR precludes any firm conclusion regarding whether reduced dendritic length or arborization is present and contributes to reduced neuropil in our subjects. Given its role in maintaining cell structure, it is plausible that changes to MAP2 protein may also contribute to reduced somal volume, another cellular change previously described in this area of cortex (Sweet et al 2004).

3.4.4 Summary

We found that 60% of subjects with Sz had dramatic reductions in MAP2-IR in BA-41, and that this deficit was correlated with reduced dendritic spine density. The loss of MAP2-IR was not explained by technical factors or subject comorbidities and treatments, suggesting MAP2-IR reduction is a disease-associated alteration. Importantly, reduced MAP2-IR was not due to a loss of MAP2 protein. Future studies will need to identify whether reduced MAP2-IR in Sz results from alterations to MAP2 phosphorylation state, conformation, and/or binding to its interaction partners. This process will be aided by identifying the affected functional domain of MAP2 that contributes to IR reduction, and by investigation of disease linked changes in the MAP2 protein interactome. Because MAP2 shares substantial sequence, regulatory, and functional homology with MAP tau, (Dehmelt and Halpain 2005) the wealth of knowledge tau biology and the rapidly expanding field of tau therapeutics(Wischik et al 2014) provide resources for identifying how MAP2 is altered in Sz and possible leads to novel therapeutics**.**

BIBLIOGRAPHY

Akil M, Pierri JN, Whitehead RE, Edgar CL, Mohila C, et al. 1999. Lamina-specific alterations in the dopamine innervation of the prefrontal cortex in schizophrenic subjects. *The American journal of psychiatry* 156: 1580-9

Allen PB, Ouimet CC, Greengard P. 1997. Spinophilin, a novel protein phosphatase 1 binding protein localized to dendritic spines. *Proceedings of the National Academy of Sciences of the United States of America* 94: 9956-61

Anderson SA, Volk DW, Lewis DA. 1996. Increased density of microtubule associated protein 2-immunoreactive neurons in the prefrontal white matter of schizophrenic subjects. *Schizophrenia research* 19: 111-9

Arnold SE, Lee VM, Gur RE, Trojanowski JQ. 1991. Abnormal expression of two microtubule-associated proteins (MAP2 and MAP5) in specific subfields of the hippocampal formation in schizophrenia. *Proceedings of the National Academy of Sciences of the United States of America* 88: 10850-4

Baddeley AVJ, EB. 2005. *Stereology for Statisticians*. pp. 69. Boca Raton, FL: Chapman & Hall/CRC.

Belanger D, Farah CA, Nguyen MD, Lauzon M, Cornibert S, Leclerc N. 2002. The projection domain of MAP2b regulates microtubule protrusion and process formation in Sf9 cells. *Journal of cell science* 115: 1523-39

Capani F, Ellisman MH, Martone ME. 2001. Filamentous actin is concentrated in specific subpopulations of neuronal and glial structures in rat central nervous system. *Brain research* 923: 1-11

Chapman J. 1966. The early symptoms of schizophrenia. *The British journal of psychiatry : the journal of mental science* 112: 225-51

Consortium SWGotPG. 2014. Biological insights from 108 schizophrenia-associated genetic loci. *Nature* 511: 421-7

Cotter D, Wilson S, Roberts E, Kerwin R, Everall IP. 2000. Increased dendritic MAP2 expression in the hippocampus in schizophrenia. *Schizophrenia research* 41: 313-23

Davare MA, Dong F, Rubin CS, Hell JW. 1999. The A-kinase anchor protein MAP2B and cAMP-dependent protein kinase are associated with class C L-type calcium channels in neurons. *The Journal of biological chemistry* 274: 30280-7

Dehmelt L, Halpain S. 2005. The MAP2/Tau family of microtubule-associated proteins. *Genome biology* 6: 204

Deo AJ, Cahill ME, Li S, Goldszer I, Henteleff R, et al. 2012. Increased expression of Kalirin-9 in the auditory cortex of schizophrenia subjects: its role in dendritic pathology. *Neurobiology of disease* 45: 796-803

Dorph-Petersen KA, Delevich KM, Marcsisin MJ, Zhang W, Sampson AR, et al. 2009. Pyramidal neuron number in layer 3 of primary auditory cortex of subjects with schizophrenia. *Brain research* 1285: 42-57

Ellman LE, Cannon TD. 2006. Interactions of genetic predisposition and intrauterine events in the etiology of schizophrenia In *The Early Course of Schizophrenia*, ed. TSPD Harvey, pp. 19-39. New York: Oxford University Press Inc.

Farah CA, Leclerc N. 2008. HMWMAP2: new perspectives on a pathway to dendritic identity. *Cell motility and the cytoskeleton* 65: 515-27

Fontaine-Lenoir V, Chambraud B, Fellous A, David S, Duchossoy Y, et al. 2006. Microtubule-associated protein 2 (MAP2) is a neurosteroid receptor. *Proceedings of the National Academy of Sciences of the United States of America* 103: 4711-6

Fromer M, Pocklington AJ, Kavanagh DH, Williams HJ, Dwyer S, et al. 2014. De novo mutations in schizophrenia implicate synaptic networks. *Nature* 506: 179-84

Fujimoto T, Tanaka H, Kumamaru E, Okamura K, Miki N. 2004. Arc interacts with microtubules/microtubule-associated protein 2 and attenuates microtubule-associated protein 2 immunoreactivity in the dendrites. *Journal of neuroscience research* 76: 51-63

Garey LJ, Ong WY, Patel TS, Kanani M, Davis A, et al. 1998. Reduced dendritic spine density on cerebral cortical pyramidal neurons in schizophrenia. *Journal of neurology, neurosurgery, and psychiatry* 65: 446-53

Glantz LA, Lewis DA. 2000. Decreased dendritic spine density on prefrontal cortical pyramidal neurons in schizophrenia. *Archives of general psychiatry* 57: 65-73

Green MF. 1996. What are the functional consequences of neurocognitive deficits in schizophrenia? *The American journal of psychiatry* 153: 321-30

Gundersen HJ. 1977. Notes on the estimation of the numerical density of arbitrary profiles: the edge effect. *Journal of Microscopy* 111: 219-23

He K, An Z, Wang Q, Li T, Li Z, et al. 2014. CACNA1C, schizophrenia and major depressive disorder in the Han Chinese population. *The British journal of psychiatry : the journal of mental science* 204: 36-9

Hermens DF, Ward PB, Hodge MA, Kaur M, Naismith SL, Hickie IB. 2010. Impaired MMN/P3a complex in first-episode psychosis: cognitive and psychosocial associations. *Progress in neuro-psychopharmacology & biological psychiatry* 34: 822-9

Hirayasu Y, McCarley RW, Salisbury DF, Tanaka S, Kwon JS, et al. 2000. Planum temporale and Heschl gyrus volume reduction in schizophrenia: a magnetic resonance imaging study of first-episode patients. *Archives of general psychiatry* 57: 692-9

Jablensky A. 2000. Epidemiology of schizophrenia: the global burden of disease and disability. *European archives of psychiatry and clinical neuroscience* 250: 274-85

Javitt DC. 2009. Sensory processing in schizophrenia: neither simple nor intact. *Schizophrenia bulletin* 35: 1059-64

Javitt DC, Shelley A, Ritter W. 2000. Associated deficits in mismatch negativity generation and tone matching in schizophrenia. *Clinical neurophysiology : official journal of the International Federation of Clinical Neurophysiology* 111: 1733-7

Javitt DC, Steinschneider M, Schroeder CE, Vaughan HG, Jr., Arezzo JC. 1994. Detection of stimulus deviance within primate primary auditory cortex: intracortical mechanisms of mismatch negativity (MMN) generation. *Brain research* 667: 192-200

Jones LB, Johnson N, Byne W. 2002. Alterations in MAP2 immunocytochemistry in areas 9 and 32 of schizophrenic prefrontal cortex. *Psychiatry research* 114: 137-48

Kapitein LC, Yau KW, Gouveia SM, van der Zwan WA, Wulf PS, et al. 2011. NMDA receptor activation suppresses microtubule growth and spine entry. *The Journal of neuroscience : the official journal of the Society for Neuroscience* 31: 8194-209

Kasai K, Shenton ME, Salisbury DF, Hirayasu Y, Onitsuka T, et al. 2003. Progressive decrease of left Heschl gyrus and planum temporale gray matter volume in first-episode schizophrenia: a longitudinal magnetic resonance imaging study. *Archives of general psychiatry* 60: 766-75

Kaufmann WE, Taylor CV, Lishaa NA. 1997. Immunoblotting patterns of cytoskeletal dendritic protein expression in human neocortex. *Molecular and chemical neuropathology / sponsored by the International Society for Neurochemistry and the World Federation of Neurology and research groups on neurochemistry and cerebrospinal fluid* 31: 235-44

Leitman DI, Laukka P, Juslin PN, Saccente E, Butler P, Javitt DC. 2010. Getting the cue: sensory contributions to auditory emotion recognition impairments in schizophrenia. *Schizophrenia bulletin* 36: 545-56

Leitman DI, Ziwich R, Pasternak R, Javitt DC. 2006. Theory of Mind (ToM) and counterfactuality deficits in schizophrenia: misperception or misinterpretation? *Psychological medicine* 36: 1075-83

Lewis DA, Lieberman JA. 2000. Catching up on schizophrenia: natural history and neurobiology. *Neuron* 28: 325-34

Lewis DA, Sweet RA. 2009. Schizophrenia from a neural circuitry perspective: advancing toward rational pharmacological therapies. *The Journal of clinical investigation* 119: 706-16

MacDonald ML, Ciccimaro E, Prakash A, Banerjee A, Seeholzer SH, et al. 2012. Biochemical fractionation and stable isotope dilution liquid chromatography-mass spectrometry for targeted and microdomain-specific protein quantification in human postmortem brain tissue. *Molecular & cellular proteomics : MCP* 11: 1670-81

Moyer CE, Delevich KM, Fish KN, Asafu-Adjei JK, Sampson AR, et al. 2012. Reduced glutamate decarboxylase 65 protein within primary auditory cortex inhibitory boutons in schizophrenia. *Biological psychiatry* 72: 734-43

Moyer CE, Delevich KM, Fish KN, Asafu-Adjei JK, Sampson AR, et al. 2013. Intracortical excitatory and thalamocortical boutons are intact in primary auditory cortex in schizophrenia. *Schizophrenia research* 149: 127-34

Moyer CE, Shelton MA, Sweet RA. 2015. Dendritic spine alterations in schizophrenia. *Neuroscience letters* 601: 46-53

Muly EC, Smith Y, Allen P, Greengard P. 2004. Subcellular distribution of spinophilin immunolabeling in primate prefrontal cortex: localization to and within dendritic spines. *The Journal of comparative neurology* 469: 185-97

Murakami K, Fellous A, Baulieu EE, Robel P. 2000. Pregnenolone binds to microtubule-associated protein 2 and stimulates microtubule assembly. *Proceedings of the National Academy of Sciences of the United States of America* 97: 3579-84

Naatanen R, Kahkonen S. 2009. Central auditory dysfunction in schizophrenia as revealed by the mismatch negativity (MMN) and its magnetic equivalent MMNm: a review. *The international journal of neuropsychopharmacology / official scientific journal of the Collegium Internationale Neuropsychopharmacologicum (CINP)* 12: 125-35

Owen MJ, Craddock N, O'Donovan MC. 2010. Suggestion of roles for both common and rare risk variants in genome-wide studies of schizophrenia. *Archives of general psychiatry* 67: 667-73

Pocklington AJ, O'Donovan M, Owen MJ. 2014. The synapse in schizophrenia. *The European journal of neuroscience* 39: 1059-67

Purcell SM, Moran JL, Fromer M, Ruderfer D, Solovieff N, et al. 2014. A polygenic burden of rare disruptive mutations in schizophrenia. *Nature* 506: 185-90

Rabinowicz EF, Silipo G, Goldman R, Javitt DC. 2000. Auditory sensory dysfunction in schizophrenia: imprecision or distractibility? *Archives of general psychiatry* 57: 1149-55

Rajarethinam R, Sahni S, Rosenberg DR, Keshavan MS. 2004. Reduced superior temporal gyrus volume in young offspring of patients with schizophrenia. *The American journal of psychiatry* 161: 1121-4

Reichenberg A, Davidson M. 2006. Cognitive functioning before or at the onset of the first episode In *The Early Course of Schizophrenia*, ed. TSPD Harvey, pp. 41-55. New York: Oxford University Press Inc.

Rioux L, Ruscheinsky D, Arnold SE. 2004. Microtubule-associated protein MAP2 expression in olfactory bulb in schizophrenia. *Psychiatry research* 128: 1-7

Ritsner MS. 2011. The clinical and therapeutic potentials of dehydroepiandrosterone and pregnenolone in schizophrenia. *Neuroscience* 191: 91-100

Rosoklija G, Keilp JG, Toomayan G, Mancevski B, Haroutunian V, et al. 2005. Altered subicular MAP2 immunoreactivity in schizophrenia. *Prilozi / Makedonska akademija na naukite i umetnostite, Oddelenie za bioloski i medicinski nauki = Contributions / Macedonian Academy of Sciences and Arts, Section of Biological and Medical Sciences* 26: 13-34

Rosoklija G, Toomayan G, Ellis SP, Keilp J, Mann JJ, et al. 2000. Structural abnormalities of subicular dendrites in subjects with schizophrenia and mood disorders: preliminary findings. *Archives of general psychiatry* 57: 349-56

Salisbury DF, Kuroki N, Kasai K, Shenton ME, McCarley RW. 2007. Progressive and interrelated functional and structural evidence of post-onset brain reduction in schizophrenia. *Archives of general psychiatry* 64: 521-9

Salyers MP, Mueser KT. 2001. Social functioning, psychopathology, and medication side effects in relation to substance use and abuse in schizophrenia. *Schizophrenia research* 48: 109-23

Sanchez C, Diaz-Nido J, Avila J. 2000. Phosphorylation of microtubule-associated protein 2 (MAP2) and its relevance for the regulation of the neuronal cytoskeleton function. *Progress in neurobiology* 61: 133-68

Schwab C, Bondada V, Sparks DL, Cahan LD, Geddes JW. 1994. Postmortem changes in the levels and localization of microtubule-associated proteins (tau, MAP2 and MAP1B) in the rat and human hippocampus. *Hippocampus* 4: 210-25

Selemon LD, Goldman-Rakic PS. 1999. The reduced neuropil hypothesis: a circuit based model of schizophrenia. *Biological psychiatry* 45: 17-25

Somenarain L, Jones LB. 2010. A comparative study of MAP2 immunostaining in areas 9 and 17 in schizophrenia and Huntington chorea. *Journal of psychiatric research* 44: 694-9

Sullivan PF, Kendler KS, Neale MC. 2003. Schizophrenia as a complex trait: evidence from a meta-analysis of twin studies. *Archives of general psychiatry* 60: 1187-92

Sweet RA, Bergen SE, Sun Z, Sampson AR, Pierri JN, Lewis DA. 2004. Pyramidal cell size reduction in schizophrenia: evidence for involvement of auditory feedforward circuits. *Biological psychiatry* 55: 1128-37

Sweet RA, Dorph-Petersen KA, Lewis DA. 2005. Mapping auditory core, lateral belt, and parabelt cortices in the human superior temporal gyrus. *The Journal of comparative neurology* 491: 270-89

Sweet RA, Henteleff RA, Zhang W, Sampson AR, Lewis DA. 2009. Reduced dendritic spine density in auditory cortex of subjects with schizophrenia. *Neuropsychopharmacology : official publication of the American College of Neuropsychopharmacology* 34: 374-89

Takahashi T, Wood SJ, Yung AR, Soulsby B, McGorry PD, et al. 2009. Progressive gray matter reduction of the superior temporal gyrus during transition to psychosis. *Archives of general psychiatry* 66: 366-76

Teng J, Takei Y, Harada A, Nakata T, Chen J, Hirokawa N. 2001. Synergistic effects of MAP2 and MAP1B knockout in neuronal migration, dendritic outgrowth, and microtubule organization. *The Journal of cell biology* 155: 65-76

Tiihonen J, Lonnqvist J, Wahlbeck K, Klaukka T, Niskanen L, et al. 2009. 11-year follow-up of mortality in patients with schizophrenia: a population-based cohort study (FIN11 study). *Lancet* 374: 620-7

Umbricht D, Koller R, Schmid L, Skrabo A, Grubel C, et al. 2003. How specific are deficits in mismatch negativity generation to schizophrenia? *Biological psychiatry* 53: 1120-31

Umbricht D, Krljes S. 2005. Mismatch negativity in schizophrenia: a meta-analysis. *Schizophrenia research* 76: 1-23

Volavka J, Cooper T, Czobor P, Bitter I, Meisner M, et al. 1992. Haloperidol blood levels and clinical effects. *Archives of general psychiatry* 49: 354-61

Wischik CM, Harrington CR, Storey JM. 2014. Tau-aggregation inhibitor therapy for Alzheimer's disease. *Biochemical pharmacology* 88: 529-39